Journal of Translational Medicine

RESEARCH

Open Access

Mitochondrial transplantation following cardiopulmonary resuscitation improves neurological function in rats by inducing M2-type MG/MΦ polarization

Jie Zhu[1†], Zhen Wang[1†], Mengda Xu[2], Xuyuan Ma[3], Maozheng Shen[3], Jingyu Yan[2] and Xiang Zhou[1,2*]

Abstract

Aim Explore the effects of mitochondrial transplantation (MT) after cardiopulmonary resuscitation (CPR) on the polarization of microglia/macrophages (MG/MΦ) and neurological function.

Methods Seventy-five Sprague-Dawley rats were randomly divided into five groups: sham, normal saline (NS), vehicle, mitochondria (Mito), and non-functional mitochondria (N-Mito) group. Rats in sham group underwent surgical procedures without cardiac arrest, while the other four groups underwent cardiac arrest and CPR, and then received NS, respiration buffer, mitochondrial suspension or non-functional mitochondria, immediately after the restoration of spontaneous circulation (ROSC). The number of mitochondria in the hippocampus, the morphology and structure of mitochondria in MG/MΦ, the phenotype of MG/MΦ, and hippocampal tissue injury, neuroinflammation, and neuronal apoptosis were detected on days 1 and 3 after ROSC. Neurodeficit score (NDS) was performed on days 1, 3, 7, 15 and 30 after ROSC.

Results Compared with other groups, the number of mitochondria in the hippocampus was increased, and the morphology and structure of mitochondria in MG/MΦ were significantly improved in the Mito group. Our results show higher expression of M2-type markers in MG/MΦ and decreased hippocampal tissue damage in the Mito group. Levels of NSE and S100β in serum, and TNF-α, IL-6 in the hippocampus were decreased, while the levels of TGF-β and IL-10 were increased in the Mito group. Apoptosis rate of neurons in the Mito group was decreased and the NDS of the Mito group was higher than the other groups.

Conclusions Exogenous MT can improve neurological function after CPR by promoting the polarization of MG/MΦ to M2-type cells, and this could be a potential method for brain protection after CPR.

Keywords Cardiac arrest, Mitochondrial transplantation, Neurological function, Microglia, Macrophages

[†]Jie Zhu and Zhen Wang contributed equally to this work and should be considered as co-first authors.

*Correspondence:
Xiang Zhou
zhouxiang188483@126.com

[1]The First School of Clinical Medicine, Southern Medical University, Guangzhou 510515, China
[2]Department of Anesthesiology, General hospital of central theater command of PLA, Wuhan 430070, China
[3]Base of Central Theater Command of People's Liberation Army, Hubei University of Medicine, Wuhan, China

Introduction

Cardiac arrest (CA) is a major threat to human health. Transient ischemia can lead to selective death of fragile neurons [1], coupled with reperfusion injury after cardiopulmonary resuscitation (CPR), making brain injury the cause of death in 73% of out-of-hospital CA cases and 27% of in-hospital CA cases [2]. Alleviate neurological dysfunction after CPR is an unmet need in the medical field. Mitochondrial transplantation (MT) is an innovative therapy to restore mitochondrial function by replacing damaged mitochondria. Studies have shown that mitochondria can persist in vivo after being transplanted via veins [3–5], arteries [6], and cerebrospinal fluid [7]. Transplanted mitochondria can be internalized by a variety of cells [8], and alleviate neuronal injury by promoting mitochondrial autophagy, reducing reactive oxygen species (ROS), mitigating neuroinflammation, and decreasing neuronal apoptosis, to improve the survival rate and neurological outcome of rats after cerebral ischemic-reperfusion injury (CIRI) [9].

The innate immune system activation and subsequent neuroinflammation are critical causes of CIRI. The activation of microglia (MG) and infiltration of circulating immune cells are the key initiators of neuroinflammation after CIRI [10]. The inflammatory cytokines and chemokines can increase the permeability of the blood-brain barrier (BBB) [11]. Peripheral macrophages (MΦ) can infiltrate the cerebral parenchyma through the damaged BBB to influence the process of neuroinflammation together with the innate immune cells in the central nervous system−MG [12]. In vivo or in vitro factors can activate MG/MΦ and differentiate them into M1 or M2 phenotypes. This process is known as MG/MΦ polarization. M1 is a pro-inflammatory type, which can produce pro-inflammatory factors and aggravate the inflammatory response. On the contrary, M2 is an anti-inflammatory type, which can produce anti-inflammatory factors to inhibit the inflammatory response and promote neuron regeneration and repair [13]. When MG are in a resting state, the cytoplasmic NF-κB binds to the Inhibitor of NF-κB (IκB) protein. When damage occurs, IκB is phosphorylated and degraded by IκB kinase. At this time, the bound NF-κB undergoes nuclear translocation, thereby promoting the transcription of many pro-inflammatory cytokine genes [14]. The activation of NF-κB signaling pathway is associated with M1 polarization of MG [15]. MG polarized to M1 can recruit leukocytes to further promote inflammation by releasing proinflammatory cytokines and chemokines [16]. Therefore, how to promote the polarization of M1 to M2 could be one protective method after CIRI. Mitochondrial function in MG/MΦ is closely related to cell polarization and neuroinflammation. Neuroinflammation can alter mitochondrial dynamics in MG/MΦ and affect mitochondria-mediated cell death pathways, while mitochondrial dysfunction can promote neuroinflammation [17]. Research has indicated that MT promotes MG polarize to M2-type and improves cognitive impairment in sepsis survivors [18]. However, the protective effect of MG/MΦ phenotypic regulation on neurological function after CPR has not been reported. We hypothesized that exogenous mitochondria could protect neurons and improve neurological function by promoting the polarization of M2-type MG/MΦ. We verified this hypothesis by establishing a CA-CPR model and transplanting gastrocnemius derived mitochondria via the femoral vein (Fig. 1).

Materials and methods

Animals

A total of 75 male Sprague-Dawley rats (weight 250–350 g, 6 to 9-week-old) were obtained from the Hunan Silaikejingda Experimental Animal Company Limited. (No.430727231102236483, Changsha, China). All animal experiments procedures were performed in compliance with the laboratory animal guideline for ethical review of animal welfare and approved by the animal experiment committee of the General Hospital of the Central Theater Command (No. 2023017).

CA-CPR model

The CA-CPR model was established as previously described [19] and following the modified Utstein-style guidelines [20]. Briefly, general anesthesia was performed by intraperitoneal injection of pentobarbital sodium. After anesthesia, a 16G venous indwelling needle was used for endotracheal intubation, a 24G venous indwelling needle connected with a pressure sensor was placed in the left femoral artery to detect mean arterial blood pressure (MAP), and a 24G venous indwelling needle placed in the right femoral venous for fluid infusion. Blood pressure, electrocardiograph, heart rate, and rectal temperature were monitored by the ALC-MPA monitor system (Alcott biotech, Shanghai, China) throughout the surgery. The asphyxial CA was induced by blocking the endotracheal tube after 10 min of mechanical ventilation. CA was identified when the systolic blood pressure (SBP) dropped to 25 mmHg [20]. Five minutes after CA, thoracic compressions and mechanical ventilation were initiated. Adrenaline (4 μg/100 g) was injected through the right femoral venous [21]. Restoration of spontaneous circulation (ROSC) was defined as spontaneous sinus rhythm and SBP > 60 mmHg maintained for at least 10 min [20]. Rodents who failed to recover spontaneous sinus rhythm within 3 min or those in which circulation could not be maintained were excluded from the study. After recovery from anesthesia, all catheters were removed and all incisions were closed after subcutaneous infiltration of 1% lidocaine. Rodents were kept alone

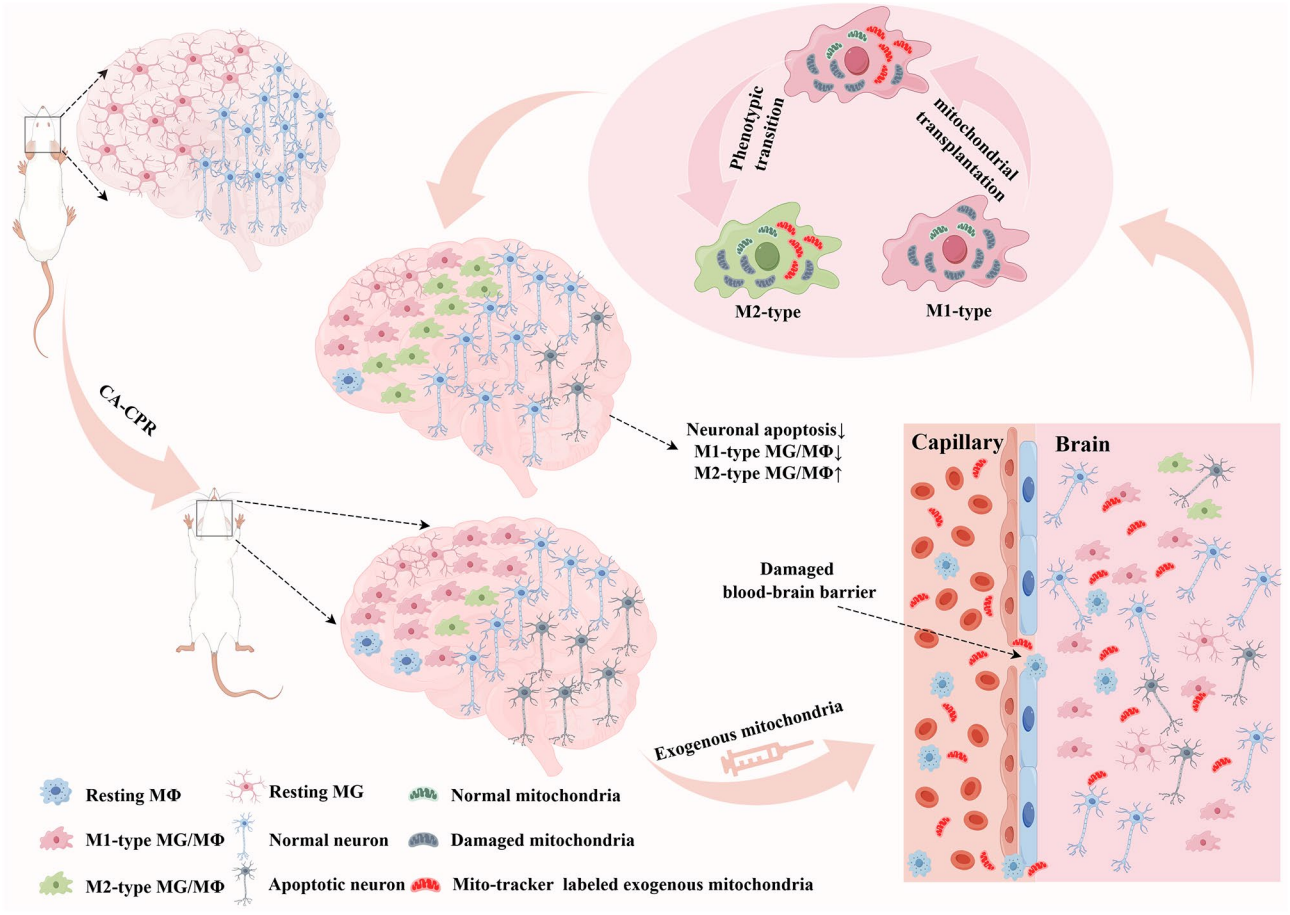

Fig. 1 Mitochondrial transplantation improves neurological function following cardiopulmonary resuscitation in rats by modulating MG/MΦ polarization. (By Figdraw)

and fed freely. Rectal temperature was maintained at 35–36 °C during surgical procedure.

Groups of rats and drug administration

The rats were numbered from 1 to 75 by body weight. Then random number method was used with Microsoft Excel software to randomly divide all the 75 animals into five groups on average: the sham group, the normal saline (NS) group, the Vehicle group, the mitochondria (Mito) group, and the non-functional mitochondria (N-Mito) group. As for the blinding, all the researchers were blind to group assignments during assessments.

Surgical procedures and mechanical ventilation were performed in rats of the sham group, and 0.5 mL of NS was injected in femoral vein 25 min after mechanical ventilation. Immediately after ROSC, the corresponding fluids were injected into the femoral vein in the other four groups: 0.5 mL of NS in the NS group, 0.5 mL of respiration buffer (250 mM sucrose, 2 mM KH_2PO_4, 10 mM $MgCl_2$, 20 mM K-HEPES, and 0.5 mM K-EGTA) in the Vehicle group, 0.5 mL of 1×10^9/mL mitochondrial suspension (contains 5×10^8 mitochondria) in the Mito group, and 0.5 mL of 1×10^9/mL frozen-thawed mitochondria in the N-Mito group. The experimental design is shown in Fig. 2.

Mitochondrial isolation, purity, activity detection, and fluorescence labeling

Gastrocnemius mitochondrial isolation

In contrast, the absolute number of mitochondria obtained from the same weight of tissues by the same method is highest in liver, second in skeletal muscle, and lowest in myocardium. However, there was no difference in cellular uptake and protective effect on target tissue among the mitochondria from different sources [22]. Therefore, after considering the operability and the degree of damage to rats, we chose gastrocnemius as the source of mitochondrial isolation.

The mitochondrial isolation protocol was performed as previously reported [23]. Briefly, fresh gastrocnemius tissues were obtained from healthy rats and rinsed with cold phosphate buffered saline (PBS). Tissues were transferred into a microcentrifuge tube, which contained 1 mL of ice-cold homogenizing buffer (300 mM sucrose, 10

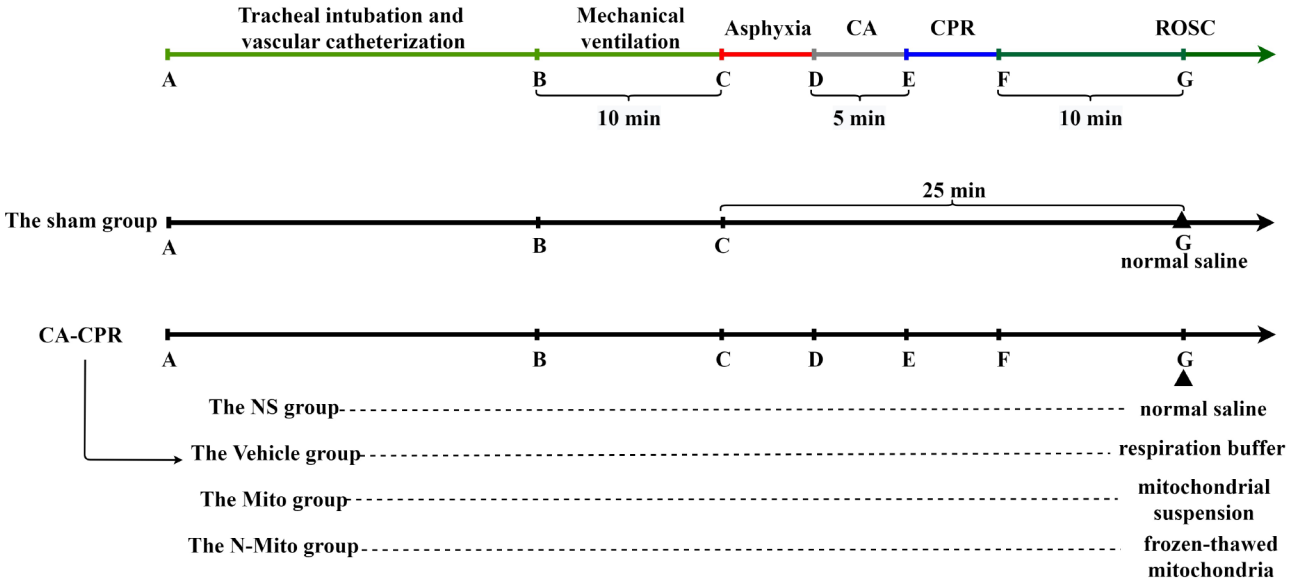

Fig. 2 Experimental design of cardiac arrest-cardiopulmonary resuscitation model

mM K-HEPES, and 1 mM K-EGTA), and then homogenized. The homogenate was replenished to 5 mL with homogenizing buffer. One milligram of Subtilisin A (P5380, Sigma-Aldrich, Darmstadt, Germany) was added into the homogenate, and incubated on ice for 10 min. Next, the homogenate was filtered through a 40 μm cell strainer and 5 mg of bovine serum albumin (ST2249, Beyotime, Shanghai, China) were added to the homogenate. It was filtered through a 40 μm, followed by a 10 μm cell strainer. The supernatants were removed after centrifugating at 9,000×g for 10 min at 4 °C. All mitochondria were suspended by 1 mL precooled respiration buffer. The amounts of mitochondria were determined by a Helber bacteria count chamber, adjusting the concentration to 1×10^9/mL. Some mitochondria were used as fresh mitochondria for subsequent transplantation. The remaining mitochondria were frozen and stored at −80 °C for over 2 weeks until subsequent use for intravenous infusion as non-functional mitochondria [8].

Analysis of mitochondrial purity by western blot

Gastrocnemius and mitochondrial proteins were extracted with RIPA lysate and PMSF. A BCA protein quantification kit (G2026-1000T, Servicebio, Wuhan, China) was used to determine total protein, and the concentration of protein was adjusted to be consistent. The loading quantity of the sample was 15 μg/well. The proteins were subjected to electrophoresis, membrane transfer, and blocking. Then, the membrane was incubated with anti-COX IV antibody (AC610, Beyotime, Shanghai, China) and anti-GAPDH antibody (LF206, Epizyme, Shanghai, China) at 4 °C overnight. Next, the membrane was washed with Tris-buffered saline with Tween 20 and incubated with horseradish peroxidase-conjugated secondary antibody (A0208, Beyotime, Shanghai, China). An ECL chemiluminescence kit (P0018S, Beyotime, Shanghai, China) was used to detect and develop the secondary antibodies.

Detection of mitochondrial viability by JC-1 staining

Mitochondrial membrane potential was detected with an enhanced mitochondrial membrane potential kit (C2003S, Beyotime, Shanghai, China) according to the manufacture instructions. The isolated mitochondria were incubated with JC-1 staining solution for 30 min at 37 °C. A fluorescence microscopy (BX53, OLYMPUS, Tokyo, Japan) was used for observation. In addition, flow cytometry was used to quantify the results. Fresh mitochondria and freeze-thawed mitochondria were incubated with JC-1 staining solution for 30 min at 37 °C respectively and detected by flow cytometry (FACSCalibur, BD Biosciences, Franklin Lakes, NJ, USA).

Labeling of mitochondria by mito-tracker red CMXRos staining

Isolated mitochondria were incubated with 50 nM preheated Mito-tracker Red CMXRos (C1049B, Beyotime, Shanghai, China) at 37 °C for 15 min, then rinsed with respiratory buffer and centrifuged at 9,000×g for 10 min at 4 °C. The mitochondria were resuspended with respiration buffer for subsequent intravenous transplantation.

Mitochondria-related detection in MG/MΦ

Co-localization of exogenous mitochondria within MG/MΦ was determine by immunofluorescence analysis on days 1, 3 and 7 after ROSC

The rats were sacrificed under deep anesthesia to obtain brains. Brain tissues were fixed with 4% paraformaldehyde

for 24 h. Sucrose gradient dehydration and OCT embedding were performed successively. Embedded tissues were frozen and sectioned (8 μm thickness). After being rewarmed, permeabilized and blocked, the sections were incubated with anti-ionized calcium-binding adapter molecule 1 (Iba1, AF7143, Beyotime, Shanghai, China) antibody at 4 °C overnight. The sections were washed with PBS and incubated with Alexa Fluor 488-conjugate secondary antibody (HZ0176, Huzhen, Shanghai, China) at room temperature for 1 h. After washing with PBS, the sections were mounted with antifade mounting medium with 4,6-diamidino-2-phenylindole (DAPI, P0131, Beyotime, Shanghai, China) for 5 min. A fluorescence microscopy was used for observation.

Detection of expression of the translocase of outer mitochondrial membrane 20 (TOMM20) in hippocampus by immunofluorescence analysis

The rats were sacrificed under deep anesthesia to obtain brain tissue on days 1 and 3 after ROSC. The brain tissues were fixed with 4% paraformaldehyde for 24 h, gradient dehydrated with ethanol, rendered transparent with xylene, and embedded with paraffin and sectioned (3 μm thickness). After dewaxing and antigen repair, the paraffin sections were used for immunofluorescence analysis. The immunofluorescence staining procedures were the same as described in 5.1. The sections were incubated with anti-TOMM20 antibody (AF5206, Affinity, Changzhou, China), followed by incubation with CY3-conjugate secondary antibody (B100802, Baiqiandu, Wuhan, China). The sections were mounted with antifade mounting medium containing DAPI, and observed by fluorescence microscopy.

Observation of mitochondrial morphology and structure in MG/MΦ by transmission electron microscopy

On days 1 and 3 after ROSC, hippocampal tissues were harvested and placed in glutaraldehyde fixing solution at 4 °C for 2–4 h, and then transferred into 1% osmium tetroxide for 2 h. After gradient dehydration, infiltration, embedding, polymerization and ultrathin section preparation, the sections were stained with 2% uranium acetate and lead citrate for 15 min. The stained sections were dried at room temperature overnight and observed using a transmission electron microscope (HT7800, Hitachi, Tokyo, Japan).

Phenotypic identification of MG/MΦ

In view of the subsequent relevant results indicating that non-functional mitochondria did not improve brain injury significantly, we did not conduct follow-up tests of MG/MΦ phenotypes in the N-Mito group.

Detection of M1-type MG/MΦ and M2-type MG/MΦ by flow cytometry

On days 1 and 3 after ROSC, hippocampal tissues were harvested. After being digested with trypsin and rinsed with PBS, cells were obtained from the hippocampus. The hippocampal cells were sequentially incubated with anti-CD86 primary antibody (ER196-01, Huabio, Hangzhou, China), CY3-conjugate secondary antibody (111-165-003, Baiqiandu, Wuhan, China), anti-CD206 primary antibody (60143-1-Ig, Proteintech, Wuhan, China) and Alexa Fluor 488-conjugate secondary antibodies (115-545-003, Baiqiandu, Wuhan, China) at 4 °C for 30 min. Frequencies of $CD86^+$ and $CD206^+$ cells were detected by flow cytometry.

Analysis of the expression of MG/MΦ marker proteins in M1-type and M2-type MG/MΦ by Western blot

Western blotting was used to examine MG/MΦ phenotypes in hippocampal tissue. The procedure of Western blot is similar to 5.1. β-actin (BS-0061R, BIOSS, Beijing, China) was used as an internal reference, and anti-CD86 antibody and anti-CD206 antibody were used as primary antibodies.

Determination of tissue damage

Determination of inflammatory cytokines in hippocampal tissues by ELISA

Hippocampal tissues were obtained on days 1 and 3 days after ROSC to determine levels of tumor necrosis factor α (TNF-α), interleukin 6 (IL-6), transforming growth factor β (TGF-β), and IL-10. Tissues were rinsed with precooled PBS, and homogenized. Homogenate was centrifugated at 5,000×g for 5 min. The supernatant was reserved for subsequent tests. Rat TNF-α, IL-6, TGF-β and IL-10 ELISA kits (MM-0180R1, MM-0190R1, MM-20594R1, MM-0195R1; Meimian, Yancheng, China) were used for TNF-α, IL-6, TGF-β and IL-10 level determination, respectively, according to the manufacture instructions. A microplate reader was used to measure the optical density.

Assessment of neuronal apoptosis rate by flow cytometry

On days 1 and 3 after ROSC, hippocampal tissues were harvested. After being digested with trypsin and rinsed with PBS, cells were obtained from the hippocampus. Apoptosis was assessed using Annexin V-FITC/PI Apoptosis Detection Kit (A211-02, Vazyme, Nanjing, China), according to the manufacture instructions. Cells were stained with propidium iodide and Annexin V-FITC at room temperature, in a dark chamber, for 15 min, and apoptosis was quantified by flow cytometry. Annexin V marked early apoptotic cells and was detected by the FITC channel, while PI marked middle-late apoptotic cells and dead cells and was detected by the PE channel.

7.3 Determination of the levels of neuron specific enolase (NSE) and central nervous system specific protein β (S100β) in serum by ELISA.

The blood samples were obtained from the abdominal aorta on days 1 and 3 after ROSC, after 2 h at room temperature were centrifugated at 3,000 rpm for 15 min, 4 °C, and serum was collected. A rat S100β ELISA kit (MM-20763R1, Meimian, Yancheng, China) and a rat NSE ELISA kit (MM-0069R1, Meimian, Yancheng, China) were used for S100β and NSE determination, according to the manufacture instructions. A microplate reader (SMR60047, USCNK, Wuhan, China) was used to measure the optical density.

Hematoxylin and eosin (H&E) staining of hippocampal tissues

The production procedures of paraffin sections were the same as 5.2. After dewaxing, the paraffin sections were successively stained with hematoxylin and eosin, dehydrated with ethanol, rendered transparent, and finally sealed with neutral balsam. An optical microscope (Eclipseci, Nikon, Tokyo, Japan) was used for observation.

Assessment of neurological function by Neurodeficit score (NDS)

NDS was performed by two researchers who were completely unaware of the experimental grouping as previously described [24]. The score included general behavior deficit, brain-stem function, motor and sensory assessments, motor behavior, behavior, and seizures. A total score of 80 indicates no injury, 0 score means brain death or death. A higher the score corresponds to a better the neurological function.

Statistical analysis

At 3 days after ROSC, the neuronal apoptosis rates in the hippocampi of the first three survived rats in the sham group and the Vehicle group were 2.83% and 35.03%, respectively. Using PASS 15.0 software, we set an error of 0.1 and a power of 80%. Accordingly, 12 was the smallest acceptable animal sample size. So, 15 animals were decided upon for each group.

Statistical analysis was performed using GraphPad Prism 8.0 software. Data were presented as mean ± standard deviation (Mean ± SD). All data shown represent a minimum of three animals. One-way ANOVA followed by Tukey's HSD was performed to test significant differences among the four groups. Repeated measurement ANOVA was applied to the analysis of NDS data. $P<0.05$ was considered to be statistically significant.

Results

Similar baseline characteristics of the groups of rats used in the CA-CPR model MAP after ROSC is decreased in CA-CPR groups compared with sham group

Among all groups, there was no significant difference in baseline characteristics before asphyxia. Asphyxia time, spontaneous heart rhythm restoration time, adrenaline dosage and mean arterial pressure immediately after ROSC were similar among the NS, Vehicle and Mito groups. Importantly, MAP immediately after ROSC was significantly decreased in the NS, Vehicle, and Mito groups compared with the sham group confirming that the CA procedure was successful. (Table 1) ECG monitoring during experiments also confirmed the CA and ROSC (Supplementary Fig. 1).

The isolated mitochondria had sufficient purity. Fresh mitochondria had good vitality, while frozen-thawed mitochondrial vitality decreased significantly

Isolated mitochondrial purity was determined by the expression of COX IV. Compared with gastrocnemius lysate, purified mitochondria expressed only COX IV and not GAPDH (a cytoplasmic marker) (Fig. 3A), indicating a successful mitochondria purification. JC-1 staining was used to detect mitochondrial membrane potential. JC-1 formed aggregates visualized as red fluorescence in healthy mitochondria, while as the membrane potential decreases, monomers are formed and visualized as

Table 1 Pre and post cardiopulmonary resuscitation characteristics of the four groups of rats

Group	sham ($n=15$)	NS ($n=15$)	Vehicle ($n=15$)	Mito ($n=15$)	*N*-Mito ($n=15$)	F value	*p* value
Weight(g)	291.79 ± 18.65	296.12 ± 15.69	291.41 ± 17.90	298.44 ± 12.29	297.89 ± 14.16	0.660	0.622
Body temperature (°C)	37.68 ± 0.36	37.53 ± 0.54	37.44 ± 0.46	37.49 ± 0.41	37.50 ± 0.51	0.581	0.677
Heart rate(bpm)	441.27 ± 19.94	426.67 ± 27.65	430.40 ± 24.69	442.53 ± 26.06	428.67 ± 26.07	1.322	0.270
Basal MAP (mmHg)	93.40 ± 5.17	93.73 ± 5.66	92.27 ± 6.11	91.40 ± 7.06	93.87 ± 4.94	0.498	0.737
MAP after mechanical ventilation (mmHg)	96.87 ± 6.12	96.80 ± 6.53	97.13 ± 4.93	96.27 ± 5.89	97.40 ± 4.15	0.086	0.987
MAP immediately after ROSC (mmHg)	97.07 ± 3.63	66.47 ± 4.42[a]	67.93 ± 5.04[a]	67.60 ± 6.30[a]	67.00 ± 4.26[a]	115.223	0.000
Asphyxia time (s)	-	229.87 ± 15.11	238.73 ± 12.24	237.00 ± 19.97	234.73 ± 19.09	0.777	0.512
Spontaneous heart rhythm restoration time (s)	-	74.80 ± 13.93	79.53 ± 16.25	75.47 ± 14.82	76.27 ± 11.87	0.323	0.809
Adrenaline dosage(μg)	-	12.93 ± 1.83	13.20 ± 2.37	13.73 ± 2.25	13.07 ± 2.49	0.365	0.779

[a] $p<0.05$ compared to the sham group

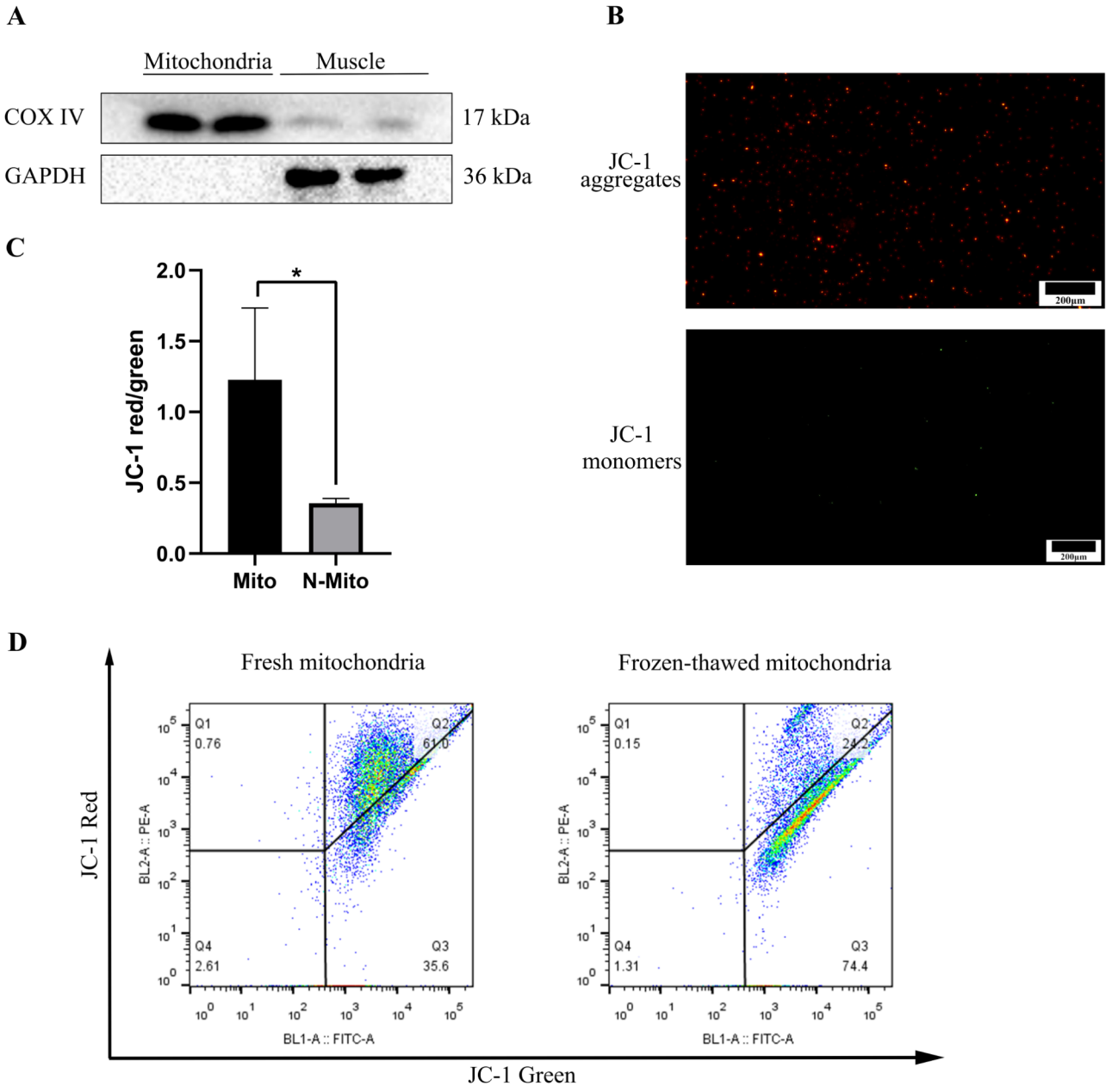

Fig. 3 Purity and vitality of isolated mitochondria. (**A**) Immunoblotting analysis of the lysate of isolated mitochondria lysate and gastrocnemius lysate. COX IV was used as a mitochondrial marker and GAPDH was used as a cytoplasmic marker ($n=4$). (**B**) Fluorescence analysis of JC-1-stained mitochondria. Red fluorescence represents JC-1aggregates, indicating higher mitochondrial membrane potential and stronger activity. Green fluorescence represents JC-1 monomers, indicating lower mitochondrial membrane potential and weaker activity (100×, $n=3$). (**C** and **D**) Flow cytometry analysis of the mitochondrial membrane potential of the isolated mitochondria stained with JC-1 indicate that the activity of frozen-thawed mitochondria was significantly lower than that of fresh mitochondria ($n=4$)

green fluorescence. The results of JC-1 staining showed that most of mitochondria were red, indicating sufficient vitality (Fig. 3B). Flow cytometry analysis of the mitochondrial membrane potential of the isolated mitochondria stained with JC-1 indicate that the activity of frozen-thawed mitochondria was significantly lower than that of fresh mitochondria (Fig. 3C and D).

Exogenous mitochondria colocalized with MG/MΦ in the hippocampus, improving the morphology and structure of mitochondria in MG/MΦ

We used Mito-tracker Red CMXRos to label isolated mitochondria and Iba1 to label MG/MΦ. Using immunofluorescence, we found transferred mitochondria in hippocampal MG/MΦ on days 1 and 3 days after ROSC. By the 7th day after ROSC, the exogenous mitochondrial

fluorescence had almost completely disappeared, which means that only a very small number of exogenous mitochondria remained in the rats at this time (Fig. 4A). At the same time points, we found increased expression of TOMM20, a marker of mitochondrial number, in the hippocampus (Fig. 4B and C). Additionally, electron microscope ultrastructure reveals that in the Sham group, the mitochondrial double membrane structure was clear and complete, and the cristae was dense. In the NS and Vehicle groups the mitochondria membranes

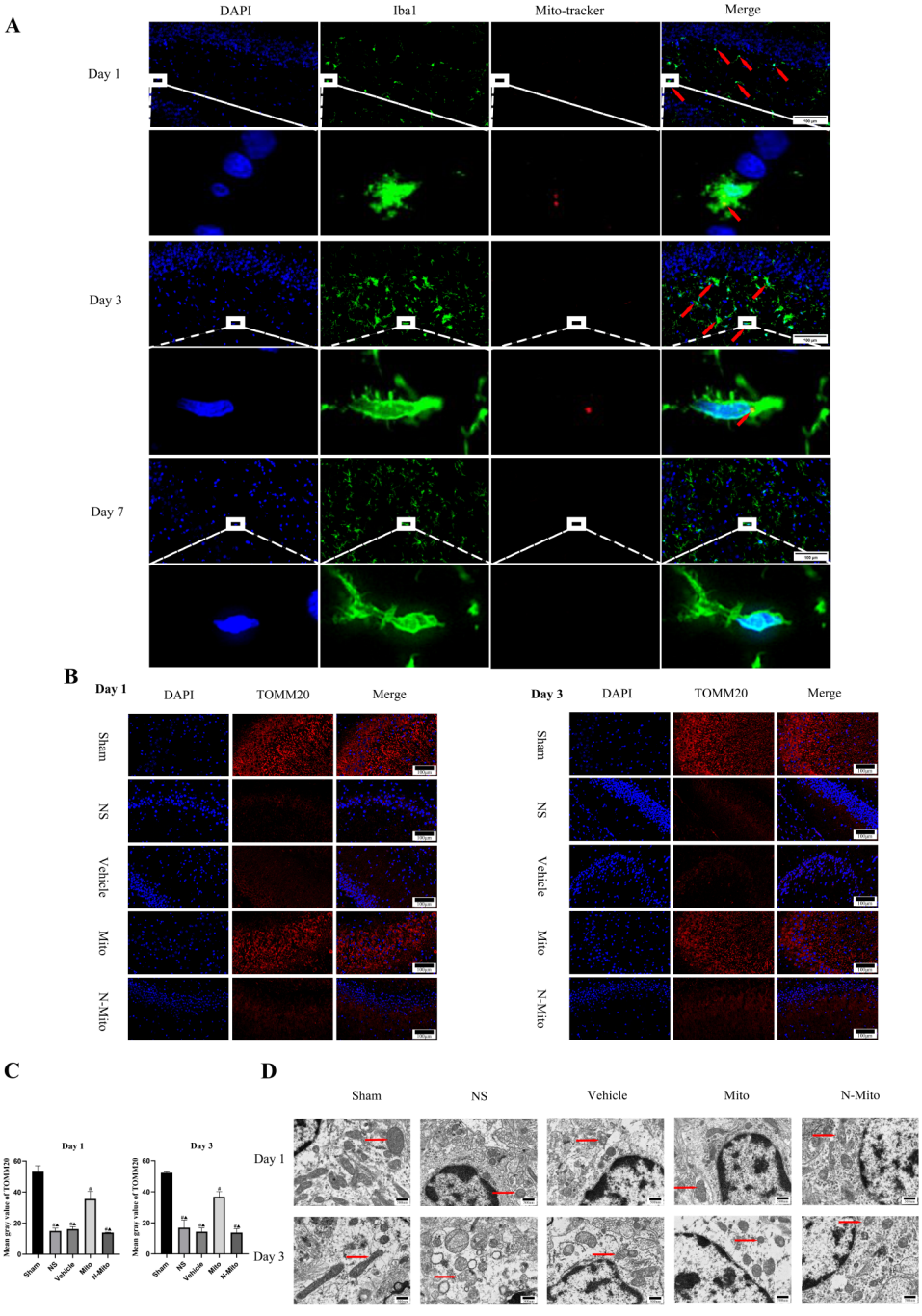

Fig. 4 Transferred mitochondria in MG/MΦ increased the number of mitochondria in hippocampus, and improved the morphology and structure of mitochondria in MG/MΦ. (**A**) Immunofluorescence analysis of mitochondria in hippocampal tissue. Green-stained cells are MG/MΦ, blue-stained regions are nuclei, and red arrows indicate the Mito-tracker Red CMXRos labeled exogenous mitochondria (400×, $n = 3$). (**B**) Immunofluorescence analysis of mitochondrial number. Blue-stained regions are nuclei, and red-stained regions are mitochondria in the hippocampus (400×, $n = 3$). (**C**) The mean gray value of TOMM20. ($n = 3$). (**D**) Morphology and structure of mitochondria in MG/MΦ were observed by electron microscopy. The red arrows indicate mitochondria; (scale bar 500 nm, $n = 3$); $^{ns}p > 0.05$; *** $p < 0.001$

were swollen and ruptured making it difficult to identify mitochondria. A large number of vacuoles and swollen mitochondrial cristae were visible. In the Mito group, the mitochondrial double membrane structure was relatively clear and complete, and the mitochondrial cristae was relatively dense and only slight swelling (Fig. 4D).

Exogenous mitochondria promoted MG/MΦ polarization to M2-type

According to the immunoblotting results, the expression of CD206, an M2-type marker of MG/MΦ, increased significantly 1 day (Fig. 5A and B) and 3 days (Fig. 5C and D) after MT, while the expression of M2-type marker CD86 was significantly decreased. Flow cytometry confirmed a

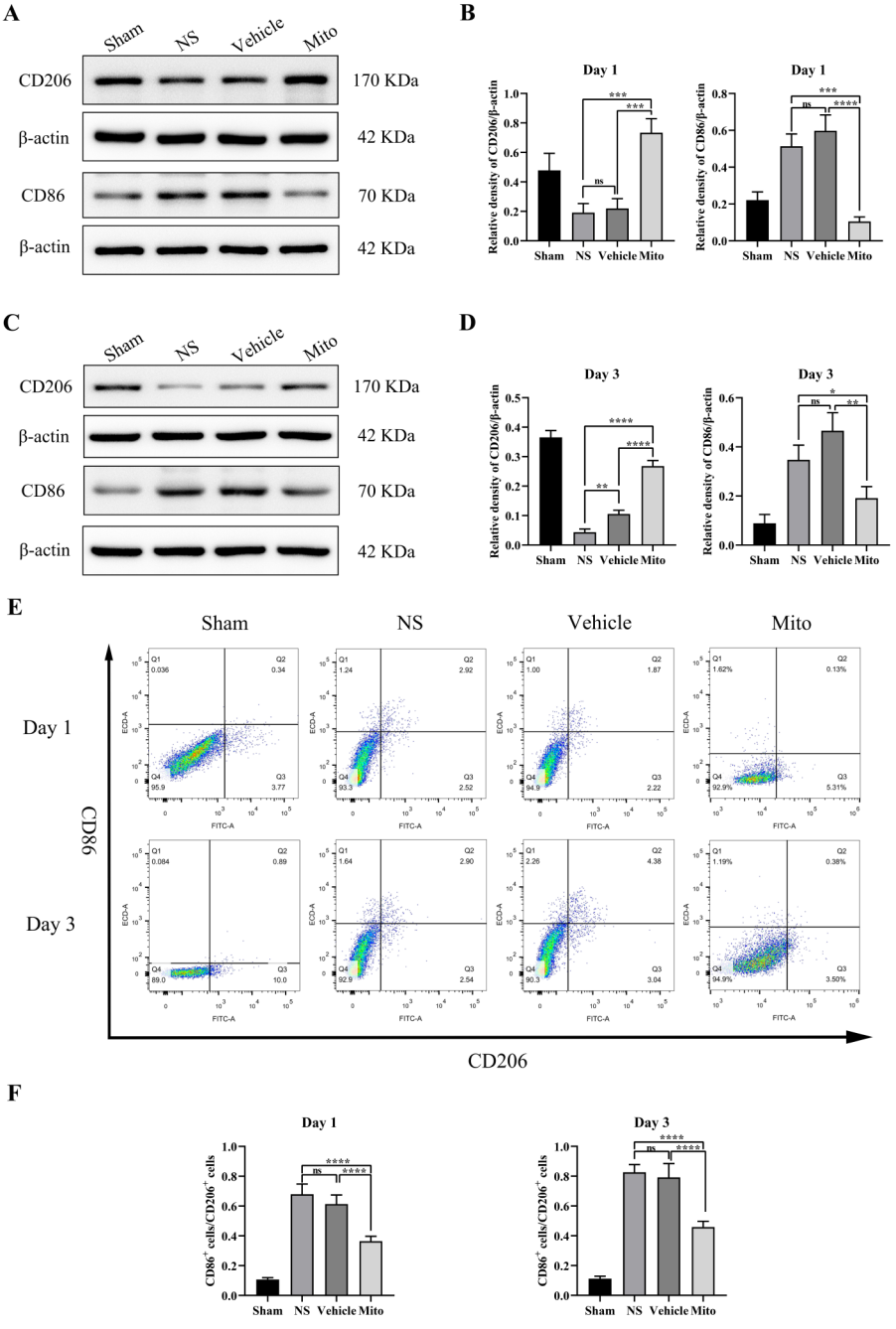

Fig. 5 Exogenous mitochondria promoted MG/MΦ polarization to M2-type. (**A**)-(**D**) Immunoblotting analysis of hippocampal tissue lysate. CD86 was used as a marker of M1-type MG/MΦ, and CD206 was used as a marker of M2-type MG/MΦ. β-actin was used as a cytoplasmic marker ($n=3$). (**A**) and (**B**) One day after ROSC. (**C**) and (**D**) Three days after ROSC. (**E**) The frequencies of MG/MΦ expressing CD86 and CD206 1 day and 3 days after ROSC were measured by flow cytometry. Q1 indicates the rate of $CD86^+$ cells, Q2 represents the cell rate in which both $CD86^+$ and $CD206^+$ are positive, and Q2 indicates the rate of $CD206^+$ cells ($n=4$). (**F**) The ratio of $CD86^+/CD206^+$ ($n=4$) $^{ns}p>0.05$; *** $p<0.001$; **** $p<0.0001$

significant reduction of $CD86^+/CD206^+$ cell ratio in the Mito group in comparison with the other groups (Fig. 5E and F). These results suggested that exogenous mitochondria promote MG/MΦ polarization to M2-type. All tests were performed in the hippocampus cells.

MT ameliorated hippocampal tissue injury

We performed H&E staining to evaluate brain damage in the different groups. In the Sham group, we found no obvious pathological damage (neurons were arranged in order, cells were lightly stained, nuclei were round). In the NS and Vehicle groups, cells were disorderly arranged, the number of neurons was decreased, and we were able to stain the nuclei. By comparison, in the Mito group, the density of neurons was increased, the arrangement was not obvious disorder, and there were fewer necrotic cells (Fig. 6A). Neuron specific enolase (NSE) and central nervous system specific protein β (S100β) can be found in sera in situations of central nervous system injury and the degree of brain injury in proportional to their levels in sera [25]. The levels of S100β and NSE were significantly lower in the Mito group than in the NS and Vehicle groups (Fig. 6B and C). In addition, flow cytometry showed that compared with the NS and Vehicle groups, neuronal apoptosis rate in the Mito group was significantly reduced (Fig. 6D and E). MG/MΦ are sensors of neuroinflammation which often exacerbates brain injury. Thus, next we measured levels of pro- and anti-inflammatory cytokines in the hippocampus. We found that proinflammatory cytokines tumor necrosis factor α (TNF-α) and interleukin 6 (IL-6) were decreased (Fig. 6F), while anti-inflammatory factors transforming growth factor β (TGF-β) and IL-10 were increased (Fig. 6G) significantly in the Mito group.

MT improves neurological function

Finally, we used NDS on days 1, 3, 7, 15 and 30 after resuscitation to evaluate rat neurological function. We found that NDS of the Mito group was higher than that of NS and Vehicle groups, suggesting that neurological dysfunction was effectively alleviated after MT (Fig. 7).

Discussion

CIRI after CPR can lead to severe neurological dysfunction and affect long-term survival [26]. MT has been shown to have promising therapeutic effects in multiple studies of brain injury [9, 27, 28]. However, most studies only focus on the direct effects of mitochondria on neurons, ignoring the indirect effects of mitochondria on other cells in the nervous system. MT has been shown to play a protective role in neurological function by improving the mitochondrial function of damaged neurons [4]. However, the regulation of MG/MΦ phenotypes by mitochondria in CA-CPR has not been reported. Our research suggested that exogenous MT promotes MG/MΦ polarization to M2-type cells, which play a protective role in neurological function after CPR.

The source of mitochondria is key to successful mitochondrial transplantation. The mitochondria for transplantation must be highly active and in sufficient numbers. Most of the early studies used autologous mitochondria for transplantation. A variety of tissues could be used as source of mitochondria with a neuroprotective role. The number of mitochondria in liver was shown to be higher than that in skeletal muscle and myocardia, but there was no significant difference in protective effect of these mitochondria [22]. Subsequently, a recent study using allogeneic mitochondria for transplantation has been reported, and good results have been obtained [29]. In combination with our experimental design, we selected allogeneic gastrocnemius muscle, which is less harmful to animals and more convenient for tissue acquisition and as a mitochondrial source. The activity of mitochondria began to decline soon after isolation. In this regard, Preble et al. proposed a tissue separation by differential centrifugation for mitochondrial extraction, which ensured that the entire extraction process was completed within 30 min, to ensure the vitality and purity of mitochondria [23]. Our research confirms the feasibility and effectiveness of this method.

Both local and systemic mitochondrial delivery can improve brain CIRI injury [6, 8, 23]. Considering that our research is a systemic ischemia-reperfusion process combined with specific clinical conditions, we chose to deliver mitochondria intravenously for a better body distribution. This method is easy to operate and clinically more acceptable. The effectiveness of intravenous mitochondrial injection has been subject of debate, with some authors arguing that isolated mitochondria cannot survive long-term in high calcium blood environment [30]. Maleki et al. reported that isolated mitochondria were not sensitive to serum calcium by conducting mitochondrial stability tests to evaluate mitochondrial swelling, mitochondrial membrane potential and hemolytic potential of isolated mitochondria after incubation with serum [31], and more than 99.95% of the mitochondria are still alive after internalization [32]. Additionally, MT has been shown to improve mitochondrial function in target organs. Jia et al. showed that intravenous injection of mitochondria can reduce the production of reactive oxygen species (ROS) in hippocampal neurons during epilepsy [4]. Pang et al. restored adenosine triphosphate (ATP) levels in lung tissue from acute lung injury by injecting mitochondria into the jugular vein [3]. Fang et al. inhibited the expression of B-cell lymph-2 (Bcl-2) and BCL2-Associated X (Bax) in spinal cord neurons of rats with spinal cord injury by injecting mitochondria into the jugular vein, thus alleviating mitochondrial dysfunction

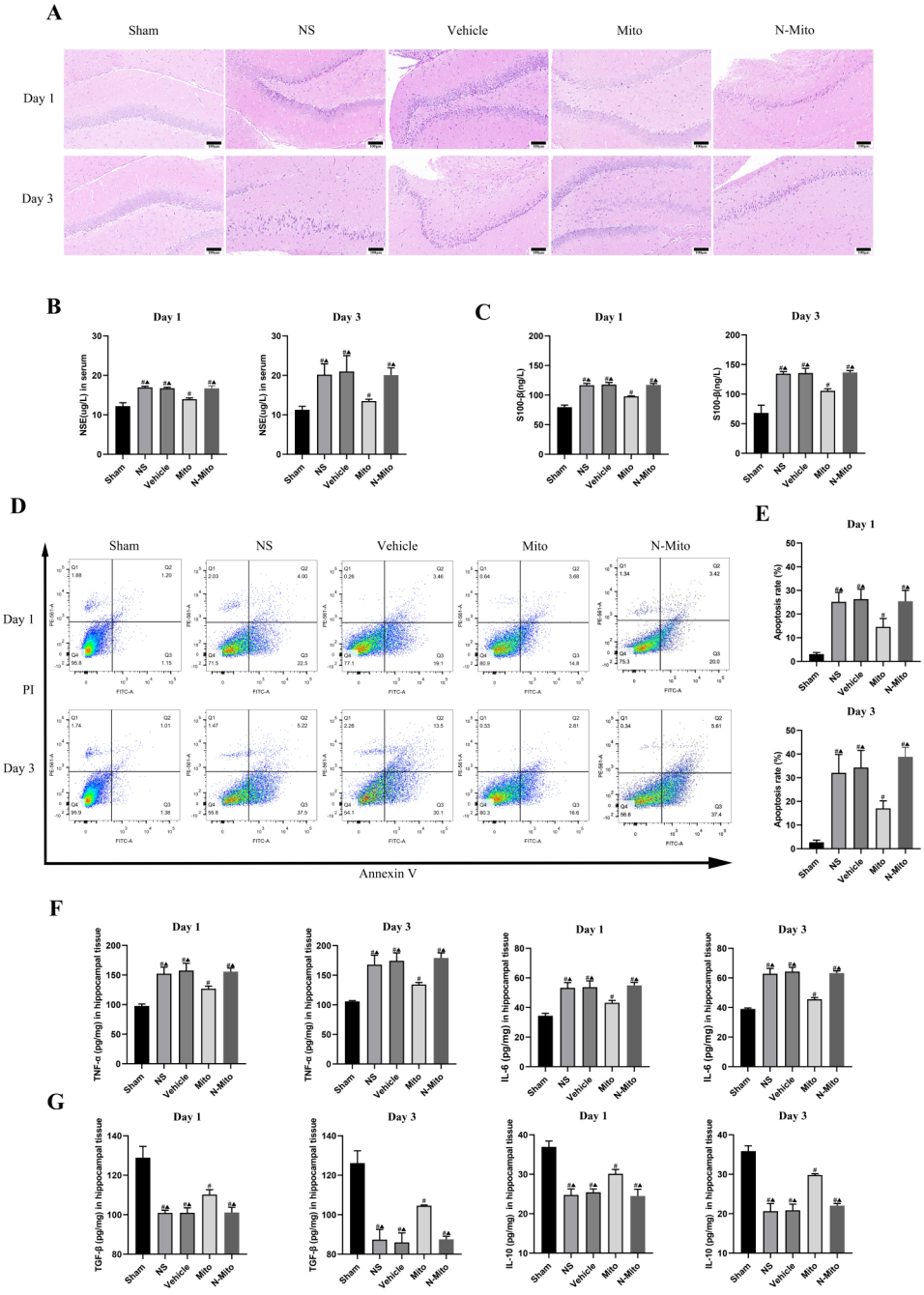

Fig. 6 Mitochondrial transplantation ameliorated hippocampal tissue injury. (**A**) Pathological examination of the hippocampus was evaluated by H&E staining (200 ×, $n = 3$). (**B**) and (**C**) The levels of NSE and S100β in the serum 1 day and 3 days after ROSC ($n = 3$). (**D**) and (**E**) Apoptosis rate of hippocampal neurons 1 day and 3 days after ROSC were determined by flow cytometry. Annexin V marked early apoptotic cells, while PI marked middle-late apoptotic cells and dead cells ($n = 4$). (**F**) and (**G**) Levels of TNF-α, IL-6, TGF-β, and IL-10 in hippocampal tissue. ($n = 3$). # : compare to the sham group; ▲: compare to the Mito group

[5]. Our study confirms the effectiveness of intravenous delivery of mitochondria.

Transplanted mitochondria can reverse neurological deficit by promoting neurogenesis in the post-stroke period, reducing cellular oxidative stress, inhibiting neuronal apoptosis [23], and alleviating neuroinflammation [4]. Resident MG and peripherally infiltrating MΦ are major participants in neuroinflammation [10]. After CIRI, the injured neurons release a variety of damaged-associated molecular patterns (DAMPs), including high mobility group box 1 (HMGB1), heat shock proteins (Hsps), peroxiredoxins-1 (Prx-1) and ATP. These DAMPs activate MG and induce secretion of proinflammatory factors that can exacerbate the inflammatory response [33]. Mitochondria are essential for cell

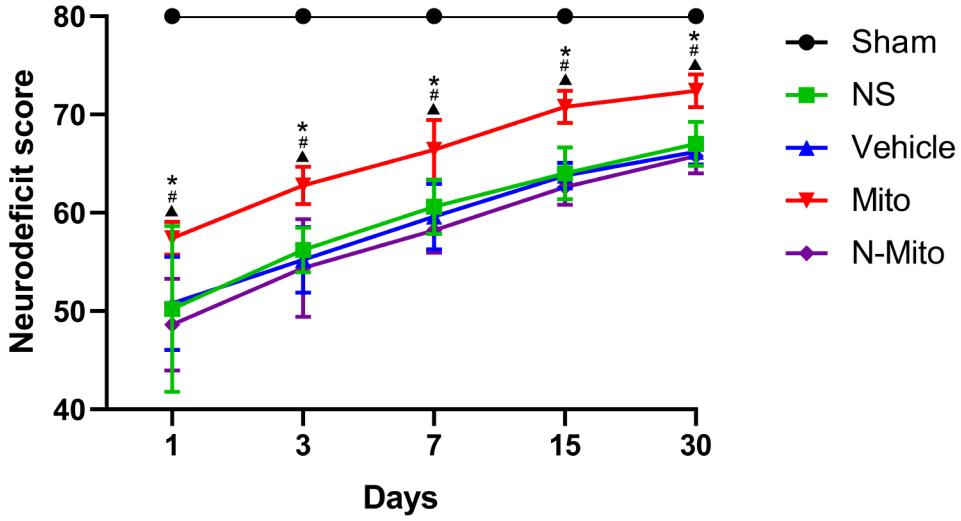

Fig. 7 Neurological deficit scores. $^{\#}p < 0.05$ compared to the Vehicle group, ▲$p < 0.05$ compared to the NS group

metabolism and function. The MG/MΦ with abnormal mitochondrial function mainly have glycolytic metabolism, while the MG/MΦ with normal mitochondrial function mainly have oxidative metabolism [34]. MG has the ability to continuously reprogram its metabolism [35]. After CA-CPR, MG/MΦ are injured by ischemia and hypoxia. At this time, mitochondrial function is impaired, and the main metabolic mode of MG/MΦ is glycolysis due to the restriction of aerobic metabolism. Notably, mitochondrial dysfunction in MG impede the activation of M2-type MG associated with tissue repair and anti-inflammatory effects [36]. Glycolysis has been shown to support the biosynthesis of proinflammatory cytokines, leading MG/MΦ to M1-type [37]. Allogeneic mitochondria transfer can restore MG metabolic gene expression, metabolite profile, and overall energy [38]. MG showed a strong ability to internalize exogenous mitochondria, and about 70% of MG cocultured with mitochondria contained a large number of internalized mitochondria, which was much higher than the internalization efficiency of other nerve cells [39]. Moreover, study has confirmed that MT can play a protective role by promoting MG/MΦ polarize to M2-type [18]. Therefore, exogenous mitochondria can effectively play a protective role by affecting MG. Our study also confirmed an increase of M2-type MG/MΦ and a decrease of neuroinflammation after MT in rats with ROSC.

The morphology and structure of mitochondria in MG/MΦ can affect the neuronal environment. Joshi et al. showed that neuroinflammation and neuronal death in neurodegenerative diseases is largely triggered by the release of dysfunctional and fragmented mitochondria by MG, and ratio between functional and dysfunctional mitochondria in the extracellular environment can influence neurologic outcomes [40]. Our results show a significant decrease in neuronal apoptosis after MT, including improvement of mitochondrial structure and reduction of neuroinflammation.

In conclusion, intravenously delivered mitochondria from gastrocnemius could reduce brain tissue injury, play a neuroprotective role, and improve nervous system prognosis. There are some limitations to our study. Exogenous mitochondria can directly act on neurons to exert brain protective effects, so MG/MΦ phenotypic transition could only be one of the brain protective mechanisms of MT after CPR. Additionally, the number of rats in each group was relatively small. And, the specific pathway and mechanism by which MG/MΦ affect neuronal apoptosis need to be further explored.

In summary, our study shows that MT improves neurological function after CPR in rats. Increased mitochondrial quantity and quality in MG/MΦ promotes M2-type polarization, which decreases inflammation, neuronal apoptosis, and brain tissue injury. Thus, our study provides support for the further studies analyzing neurological function protection after CPR.

Supplementary Information

The online version contains supplementary material available at https://doi.org/10.1186/s12967-024-05815-2.

Supplementary Material 1

Acknowledgements
We thank LetPub (www.letpub.com) for linguistic assistance and pre-submission expert review.

Author contributions
XZ and JZ contributed to the conception and design. JZ, ZW, MX, XM and MS designed and/or performed experiments. JZ, ZW and JY contributed to the acquisition of data or analysis and interpretation of data. XZ, JZ, and ZW drafted the article. All authors read and approved the final version of this manuscript.

Funding
This work was supported by the National Natural Science Foundation of China (82372210, 81901932) and Natural Science Foundation of Hubei Province (2021CFB492).

Data availability
The datasets generated and analyzed during this study are available from the corresponding author upon reasonable request.

Declarations

Ethics approval and consent to participate
Not applicable.

Consent for publication
All listed authors consent to the submission, and all data are used with the consent of the person generating the data.

Competing interests
The authors declare that they have no competing interests.

Received: 22 May 2024 / Accepted: 29 October 2024
Published online: 11 November 2024

References

1. Sun W, et al. A modified four vessel occlusion model of global cerebral ischemia in rats. J Neurosci Methods. 2021;352:109090.
2. Witten L, et al. Reasons for death in patients successfully resuscitated from out-of-hospital and in-hospital cardiac arrest. Resuscitation. 2019;136:93–9.
3. Pang YL, et al. Viable allogeneic mitochondria transplantation improves Gas Exchange and alveolar-capillary permeability in rats with Endotoxin-Induced Acute Lung injuries. Int J Med Sci. 2022;19:1036–46.
4. Jia X, et al. Mitochondrial transplantation ameliorates hippocampal damage following status epilepticus. Anim Model Exp Med. 2023;6:41–50.
5. Fang SY, et al. Transplantation of viable mitochondria attenuates neurologic injury after spinal cord ischemia. J Thorac Cardiovasc Surg. 2021;161:e337–47.
6. Kubat GB, et al. Investigation of the effect of isolated mitochondria transplantation on renal ischemia-reperfusion injury in rats. Toxicol Appl Pharmacol. 2021;433:115780.
7. Ma H, et al. Transplantation of platelet-derived mitochondria alleviates cognitive impairment and mitochondrial dysfunction in db/db mice. Clin Sci (Lond). 2020;134:2161–75.
8. Hayashida K, et al. Exogenous mitochondrial transplantation improves survival and neurological outcomes after resuscitation from cardiac arrest. Bmc Med. 2023;21:56.
9. Pourmohammadi-Bejarpasi Z, et al. Mesenchymal stem cells-derived mitochondria transplantation mitigates I/R-induced injury, abolishes I/R-induced apoptosis, and restores motor function in acute ischemia stroke rat model. Brain Res Bull. 2020;165:70–80.
10. Sandroni C, Cronberg T, Sekhon M. Brain injury after cardiac arrest: pathophysiology, treatment, and prognosis. Intensive Care Med. 2021;47:1393–414.
11. Guo X, Liu R, Jia M, Wang Q, Wu J. Ischemia Reperfusion Injury Induced Blood Brain Barrier Dysfunction and the involved molecular mechanism. Neurochem Res. 2023;48:2320–34.
12. Li Q, Barres BA. Microglia and macrophages in brain homeostasis and disease. Nat Rev Immunol. 2018;18:225–42.
13. Wang Q, et al. Microglia polarization in Alzheimer's Disease: mechanisms and a potential therapeutic target. Front Aging Neurosci. 2021;13:772717.
14. Zhang S, et al. Protective effect of flavonoid-rich extract from Rosa laevigata Michx on cerebral ischemia-reperfusion injury through suppression of apoptosis and inflammation. Neurochem Int. 2013;63:522–32.
15. Kong L, et al. mtDNA-STING Axis mediates microglial polarization via IRF3/NF-kappaB signaling after ischemic stroke. Front Immunol. 2022;13:860977.
16. Lai AY, Todd KG. Microglia in cerebral ischemia: molecular actions and interactions. Can J Physiol Pharmacol. 2006;84:49–59.
17. van Horssen J, van Schaik P, Witte M. Inflammation and mitochondrial dysfunction: a vicious circle in neurodegenerative disorders? Neurosci Lett. 2019;710:132931.
18. Yan C, et al. Mitochondrial transplantation attenuates brain dysfunction in Sepsis by driving microglial M2 polarization. Mol Neurobiol. 2020;57:3875–90.
19. Zhou X, et al. Cyclosporine A plus ischemic postconditioning improves neurological function in rats after Cardiac Resuscitation. Neurocrit Care. 2020;32:812–21.
20. Idris AH, et al. Utstein-style guidelines for uniform reporting of laboratory CPR research. A statement for healthcare professionals from a Task Force of the American Heart Association, the American College of Emergency Physicians, the American College of Cardiology, the European Resuscitation Council, the Heart and Stroke Foundation of Canada, the Institute of Critical Care Medicine, the Safar Center for Resuscitation Research, and the Society for Academic Emergency Medicine. Resuscitation. 1996;33:69–84.
21. Chen MH, Lu JY, Xie L, Zheng JH, Song FQ. What is the optimal dose of epinephrine during cardiopulmonary resuscitation in a rat model? Am J Emerg Med. 2010;28:284–90.
22. McCully JD, Levitsky S, Del NP, Cowan DB. Mitochondrial transplantation for therapeutic use. Clin Transl Med. 2016;5:16.
23. Preble JM et al. Rapid isolation and purification of mitochondria for transplantation by tissue dissociation and differential filtration. J Vis Exp. 2014;91:e51682.
24. Geocadin RG, et al. A novel quantitative EEG injury measure of global cerebral ischemia. Clin Neurophysiol. 2000;111:1779–87.
25. Ekmektzoglou KA, Xanthos T, Papadimitriou L. Biochemical markers (NSE, S-100, IL-8) as predictors of neurological outcome in patients after cardiac arrest and return of spontaneous circulation. Resuscitation. 2007;75:219–28.
26. Yan S, et al. The global survival rate among adult out-of-hospital cardiac arrest patients who received cardiopulmonary resuscitation: a systematic review and meta-analysis. Crit Care. 2020;24:61.
27. Nakamura Y, Lo EH, Hayakawa K. Placental Mitochondria Therapy for Cerebral Ischemia-Reperfusion Injury in mice. Stroke. 2020;51:3142–6.
28. Zhang B, et al. Effects of Brain-Derived Mitochondria on the function of Neuron and Vascular endothelial cell after traumatic brain Injury. World Neurosurg. 2020;138:e1–9.
29. Chang JC, et al. Allogeneic/xenogeneic transplantation of peptide-labeled mitochondria in Parkinson's disease: restoration of mitochondria functions and attenuation of 6-hydroxydopamine-induced neurotoxicity. Transl Res. 2016;170:40–56.
30. Bertero E, O'Rourke B, Maack C. Mitochondria do not survive calcium overload during transplantation. Circ Res. 2020;126:784–6.
31. Maleki F, Rabbani S, Shirkoohi R, Rezaei M. Allogeneic mitochondrial transplantation ameliorates cardiac dysfunction due to doxorubicin: an in vivo study. Biomed Pharmacother. 2023;168:115651.
32. Masuzawa A, et al. Transplantation of autologously derived mitochondria protects the heart from ischemia-reperfusion injury. Am J Physiol Heart Circ Physiol. 2013;304:H966–82.
33. Gülke E, Gelderblom M, Magnus T. Danger signals in stroke and their role on microglia activation after ischemia. Ther Adv Neurol Disord. 2018;11:1276995822.
34. Sun XR, Yao ZM, Chen L, Huang J, Dong S. Y. metabolic reprogramming regulates microglial polarization and its role in cerebral ischemia reperfusion. Fundam Clin Pharmacol. 2023;37:1065–78.
35. Neher JJ, Cunningham C. Priming Microglia for Innate Immune memory in the brain. Trends Immunol. 2019;40:358–74.
36. Ferger AI, et al. Effects of mitochondrial dysfunction on the immunological properties of microglia. J Neuroinflammation. 2010;7:45.
37. Zhang S, et al. Immunometabolism of phagocytes and relationships to Cardiac Repair. Front Cardiovasc Med. 2019;6:42.
38. Wu TH, et al. Mitochondrial transfer by Photothermal Nanoblade restores Metabolite Profile in mammalian cells. Cell Metab. 2016;23:921–9.
39. Zhao J, et al. Mitochondria transplantation protects traumatic brain injury via promoting neuronal survival and astrocytic BDNF. Transl Res. 2021;235:102–14.
40. Joshi AU, et al. Fragmented mitochondria released from microglia trigger A1 astrocytic response and propagate inflammatory neurodegeneration. Nat Neurosci. 2019;22:1635–48.

Publisher's note